Trenchless Technology Research

Point vibration measurements for the detection of shallow-buried objects

J.M. Muggleton [a], M.J. Brennan [b], C.D.F. Rogers [c,*]

[a] Institute of Sound & Vibration Research, University of Southampton, Highfield, Southampton SO17 1BJ, UK
[b] Departamento do Engenharia Mecânica, UNESP, Ilha Solteira, SP 15385-000, Brazil
[c] School of Civil Engineering, University of Birmingham, Edgbaston, Birmingham B15 2TT, UK

A B S T R A C T

A major UK initiative, entitled 'Mapping the Underworld', is seeking to address the serious social, environmental and economic consequences arising from an inability to locate accurately and comprehensively the buried utility service infrastructure without resorting to extensive excavations. Mapping the Underworld aims to develop and prove the efficacy of a multi-sensor device for accurate remote buried utility service detection, location and, where possible, identification. One of the technologies to be incorporated in the device is low-frequency vibro-acoustics, and application of this technique for detecting buried infrastructure is currently being investigated. Here, the potential for making a number of simple point vibration measurements in order to detect shallow-buried objects, in particular plastic pipes, is explored. Point measurements can be made relatively quickly without the need for arrays of surface sensors, which can be expensive, time-consuming to deploy, and sometimes impractical in congested areas.

At low frequencies, the ground behaves as a simple single-degree-of-freedom (mass–spring) system with a well-defined resonance, the frequency of which will depend on the density and elastic properties of the soil locally. This resonance will be altered by the presence of a buried object whose properties differ from the surrounding soil. It is this behavior which can be exploited in order to detect the presence of a buried object, provided it is buried at a sufficiently shallow depth. The theoretical background is described and preliminary measurements are made both on a dedicated buried pipe rig and on the ground over a domestic waste pipe. Preliminary findings suggest that, for shallow-buried pipes, a measurement of this kind could be a quick and useful adjunct to more conventional methods of buried pipe detection.

© 2012 Elsevier Ltd. Open access under CC BY license.

1. Introduction

The problems associated with inaccurate location of buried pipes and cables have been serious for many years and are getting worse as a result of increasing traffic congestion in the UK's major urban areas. The problems primarily derive from the fact that the vast majority of the buried utility infrastructure exists beneath roads and therefore any excavation is likely to disrupt the traffic. A recent UK study estimated that street works cost the UK £7 bn annually; comprising £5.5 bn in social and indirect costs and £1.5 bn in direct costs (McMahon et al., 2005).

The location techniques that are currently commercially available are either simple (yet strictly limited in their ability to detect the wide variety of utilities) and carried out immediately prior to excavation by site operatives or are more sophisticated and carried out by specialist contractors. Controlled trials carried out by UK Water Industry Research have shown that, even when sophisti-

cated detection techniques are employed, detection rates are often poor (Ashdown, 2000) and, as a result, far more excavations are carried out than would otherwise be necessary for maintenance and repair. While a variety of techniques using different technologies are available, all suffer from the same essential drawback that, when deployed alone, they will not provide an adequate solution to the problem; moreover, all have their own specific limitations.

In response to this, a large multi-center programme, Mapping the Underworld (2011), is being undertaken in the UK to assess the feasibility of a range of potential technologies that can be combined into a single device to accurately locate buried pipes and cables. The potential technologies include ground penetrating radar, low-frequency quasi-static electromagnetic fields, passive magnetic fields and low frequency vibro-acoustics and significant advances have already been made (Royal et al., 2010, 2011). In this paper, the focus is low-frequency vibro-acoustics, in particular the detection of shallow-buried pipes.

Low-frequency vibro-acoustic methods have been researched and developed previously for the detection of shallow underground objects, particularly in the military context, such as the detection of landmines buried close to the surface. Xiang and

* Corresponding author. Tel.: +44 121 414 5066; fax: +44 121 414 3675.
E-mail addresses: jm9@soton.ac.uk (J.M. Muggleton), c.d.f.rogers@bham.ac.uk (C.D.F. Rogers).

Sabatier (2002, 2003) developed a laser doppler vibrometer-based system in which the ground around a suspected target is insonified by loudspeakers and the ground surface vibration measured simultaneously. The aim is to induce resonance in the landmine which will then manifest as an increase in vibration velocity directly above the mine. A ground surface vibration image, typically covering an area of 1 m², is then used to ascertain the mine location. However, laser Doppler systems are expensive, often cumbersome and not suitable for all surface types (Muggleton and Brennan, 2010). Another implementation of this resonance-based system was developed by Scott et al. (2001) in which the ground excitation was provided by Rayleigh surface waves generated by an electro-dynamic shaker. They used an array of contact sensors to determine the location with the maximum vibration amplitude. An alternative method has been developed by Gucunski et al. (2000). They suggest a wave-based method in which, again, Rayleigh surface waves are used to excite the ground. Objects buried close to the ground surface will affect the wave dispersion, producing measureable fluctuations in the phase velocity. As for the previous methods, an array of surface transducers is required. In addition, however, inversion of the phase curve is required to compute the phase velocity, which can be numerically unstable, and the results can be difficult to interpret.

Fortunately, the requirements for civil applications are far less stringent than those for military ones (such as the requirements to operate at significant standoff and to achieve high advance rates). Here, the potential for making a number of simple point vibration measurements, which reveal the elastic properties of the ground locally in order to detect shallow-buried objects, is explored. Point measurements can be made relatively quickly without the need for arrays of surface sensors, which can be expensive, time-consuming to deploy, and sometimes impractical in congested areas. Data analysis and interpretation can be relatively quick and simple, potentially enabling operators without in-depth knowledge of vibro-acoustics to exploit the technology.

The structure of this paper is organized as follows: Section 2 describes the background to the method and its rationale, and presents analytic expressions for the key parameters of interest. In Section 3, measurements made on a dedicated pipe rig are described and the results presented. Section 4 describes measurements made over a live domestic drain. Finally, in Section 5, some conclusions are drawn and possible ways ahead discussed.

2. Background

2.1. Excitation of the ground

Consider the ground as a homogeneous elastic half space, excited by a harmonic vertical load, f, acting over a circular area with radius a, as shown in Fig. 1. Harding and Sneddon (1945) give the local static stiffness, k, (force, f, divided by displacement, x at zero frequency) as

$$k = \frac{f}{x} = \frac{2Ea}{1 - v^2} \tag{1}$$

where E and v are the elastic modulus and Poisson's ratio of the ground respectively.

Additionally, for dynamic excitation at frequencies greater than zero, there will be a mass component resulting from the mass of the moving part of the exciter and the attached, or radiation, mass. The radiation mass has a similar effect to that of a baffled piston (Kinsler et al., 1982), giving the total mass at low frequencies, m, as

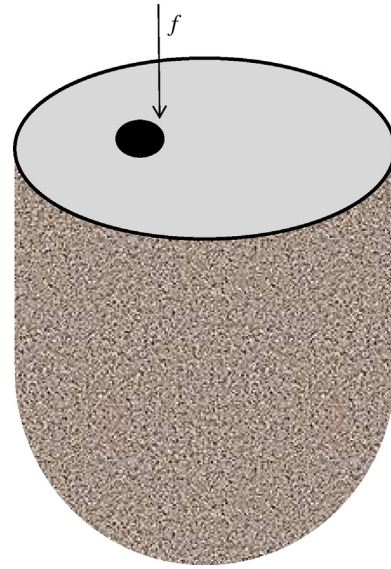$$m = \pi a^2 \left(\rho_e l + \rho \frac{8a}{3\pi} \right) \tag{2}$$

Fig. 1. The ground as an elastic half-space.

where ρ is the density of the soil, ρ_e is the density of the exciter piston, and l is its length. Finally, there will be a damping component arising from the radiation of power into the ground from the excitation point (Pinnington, 1988; Miller and Pursey, 1954).

This system comprising mass, stiffness and damping components can now be seen clearly to be a classical single-degree-of-freedom system, as shown in Fig. 2.

The equation of motion of this system is given by

$$m\ddot{x} + c\dot{x} + kx = f \tag{3}$$

where f is the applied force, m is the mass, k is the spring stiffness, c is the damping and where the dot and double dot denote differentiation with respect to time once and twice respectively.

Assuming harmonic excitation so that $f = Fe^{j\omega t}$ and $x = Xe^{j\omega t}$ ($\ddot{x} = \ddot{X}e^{j\omega t}$), the frequency domain quantity, point acceleration (acceleration/force) is therefore given by

$$\frac{\ddot{X}}{F} = \frac{1}{m - \frac{k}{\omega^2} - i\frac{c}{\omega}} \tag{4}$$

where ω is the angular frequency. A typical acceleration plot is shown in Fig. 3, revealing a well-defined resonance.

The resonance frequency (the frequency of maximum amplitude) is given by

$$\omega_R = \omega_n \sqrt{1 + 2\varsigma^2} \tag{5}$$

also shown in the figure, where ω_n is the undamped natural frequency given by

$$\omega_n = \sqrt{\frac{k}{m}} \tag{6}$$

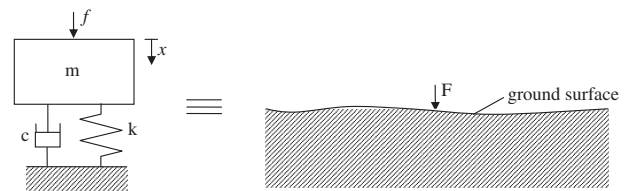and ζ is the damping ratio given by $\zeta = \frac{c}{2m\omega_n}$.

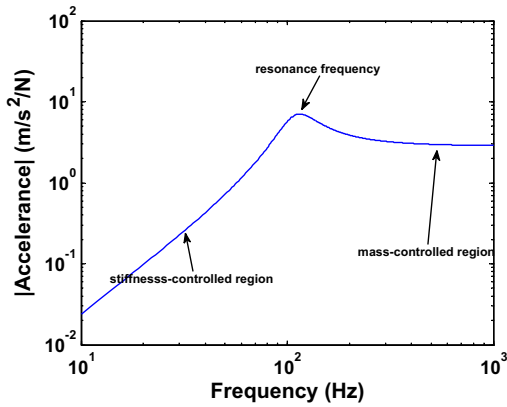**Fig. 2.** The ground as a single-degree-of-freedom system.

Fig. 3. Typical accelerance plot (here only the magnitude of the accelerance is shown) (values of $m = 0.35$, $k = 1.67 \times 105$ and $c = 100$ were used here).

Well below and well above the resonance frequency, the accelerance is given by $|\frac{\ddot{X}}{F}| = \frac{\omega^2}{k}$ and $|\frac{\ddot{X}}{F}| = \frac{1}{m}$ respectively, giving the stiffness- and mass-controlled regions shown in the figure.

Returning to the case of ground excitation considered here, substituting Eqs. (1) and (2) into Eq. (6) gives the undamped natural frequency ω_n as

$$\omega_n = \sqrt{\frac{2E}{\pi at(\rho_e l + \rho \frac{8a}{3\pi})(1 - v^2)}} \qquad (7)$$

It can be seen that this is dependent not only on the elastic properties of the soil, E, ρ and v, but also on the excitation radius, a; the larger the excitation radius, the lower the natural frequency.

2.2. Effect of a shallow-buried object

In the presence of a shallow-buried object, the mass–spring behavior will be altered according to the elastic properties of the object. The ground stiffness locally will be modified by the stiffness of the object; possibly the radiation mass may be altered if there are changes in the ground conditions very close to the surface; the damping characteristics are also likely to change. It is anticipated that it may be possible to detect a shallow-buried object by observing changes in the resonance behavior measured directly above the object compared with measurements made locally around it. These changes could include both the resonance frequency itself and the magnitude of the response at resonance.

2.2.1. Region of influence

It is possible to estimate (to an order of magnitude at least) the depth to which an object could potentially be buried and detected by these means. Consider the stiffness term given in Eq. (1). A grounded, but laterally unconstrained circular column of soil of radius a and length L has a stiffness of $\frac{E\pi a^2}{L(1-v^2)}$. Comparing this with Eq. (1) indicates that the depth of soil contributing to the vertical stiffness measured at the ground surface is of the order of $\pi a/2$. It might be expected, therefore, that objects buried at depths of this *order of magnitude* would influence the measured stiffness at the ground surface and hence the measured resonance, thus potentially enabling their detection. Moreover, it suggests that the larger the excitation radius, the greater the depths at which objects could be detected.

3. Experimental measurements on a dedicated pipe rig

3.1. Description of experimental rig

Initially, measurements were made on a small dedicated pipe rig. The rig comprises two 3 m lengths of high density polyethylene (HDPE) pipe, joined together at right angles and buried at a depth of approximately 30 cm. At each end, additional elbows bring the pipe up to the surface. For these preliminary tests the pipe contained air only, as the stiffness of an air-filled pipe will differ more from the stiffness of soil than would a water-filled pipe. The pipe parameters are shown in Table 1.

The pipe was laid on a thin layer of sand and then the original soil, classified as silty sand (80% sand, 20% silt), was returned to the trench. The pipe was buried for about a year before the measurements were made, so the soil around the pipe was well consolidated. Fig. 4 shows the pipe just prior to burial.

3.2. Experimental measurements on test rig

A Wilcoxon F4/Z820WA (Wilcoxon, 2011) electrodynamic shaker (Fig. 5) was used to excite the ground vertically, by placing it directly on the ground. This exciter has a built in impedance head which senses both the applied force and the measured acceleration, enabling straightforward computation of the accelerance without the need for additional sensors. The shaker piston has a mass of 140 g and a contact diameter of approximately 5 cm.

Table 1
Pipe parameters.

Pipe material	Black PE100
Outer diameter (mm)	110
Wall thickness (mm)	6.6
Elastic modulus (N/m²)	3×10^9
Density (kg/m³)	900–1000

Fig. 4. Pipe rig just prior to burial.

Fig. 5. Electrodynamic shaker (here on a gravel surface).

Point accelerance measurements were made along six 2 m-long lines crossing the pipe at right-angles. Measurements were made at approximately 10 cm intervals along each line, resulting in 21 measurement locations per line. The approximate location of the lines is shown in Fig. 6. The setup for one line is shown in Fig. 7.

A sweep input to the shaker was used, with a frequency range from 10 Hz to 800 Hz, and with a duration of approximately 30 s. A 2 kHz sampling rate was employed for the data acquisition, with a total acquisition time of 32.768 s. A Prosig P8020, 24-bit data acquisition system was used to capture the data.

For each measurement, the point accelerance was computed from the ratio of two cross spectra: that of the measured acceleration and the voltage applied to the shaker and that of force delivered by the shaker and the voltage applied to it.

$$\text{Point accelerance} = \frac{G_{AV}}{G_{FV}} \qquad (8)$$

where the subscripts A, F and V refer to the measured acceleration, the force delivered by the shaker and the input voltage respectively.

3.3. Test results

Fig. 8 shows the point accelerance for a representative measurement location not directly above the pipe as well as one directly over the pipe along the same measurement line.
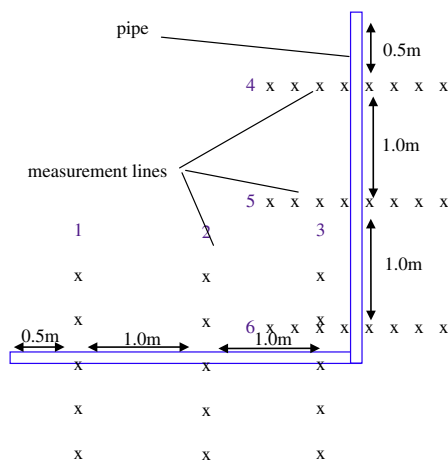

Fig. 6. Location of measurement lines (the crosses are for illustrative purposes only and do not necessarily represent the actual number of measurement positions along a line).
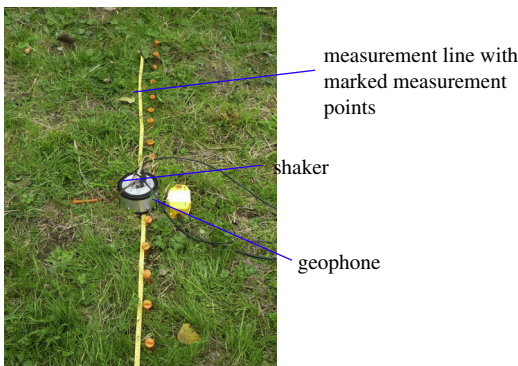

Fig. 7. Setup for the measurement of point accelerance with marked measurement positions (in this photograph an additional geophone is also present adjacent to the shaker).
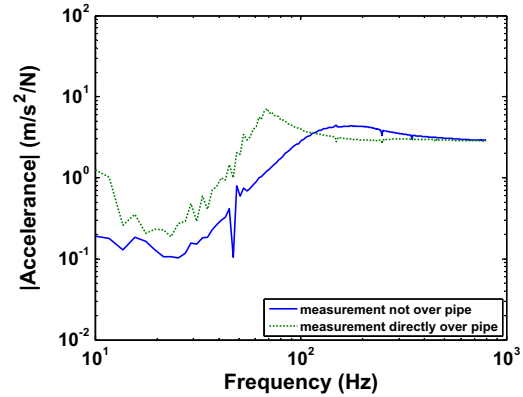

Fig. 8. Two point accelerance measurements (the peaks at 50 Hz are associated with mains interference).

For the measurement not over the pipe, the anticipated mass–spring response can be clearly seen, with the well-damped resonance at a frequency of approximately 170 Hz. For the measurement over the pipe, it can be seen that the resonance frequency reduces to around 70 Hz, which indicates that either the local stiffness has reduced or the mass has increased. Inspection of the low- and high-frequency asymptotes suggests that the mass has not changed, but it is the stiffness which has altered, as anticipated. The high-frequency mass lines indicate a mass of approximately 300–350 g; 140 g of this can be attributed to the shaker piston, with the remaining 160–210 g being the radiation mass contribution. From Eq. (2) the expected radiation mass (assuming a soil density of 2000 kg/m^3) is approximately 80 g, so 160–210 g is rather more than anticipated. However, Eq. (2) relates to a fluid only, so the effects of shear are not included; this may account for the observed difference. In addition to the reduction in resonance frequency it can be seen that the peak height of the resonance peak is higher for the measurement point directly above the pipe (by approximately 65% in this case), indicating that the damping has altered slightly as well. Fig. 9a–h shows the mass–spring resonance frequency plotted against distance along the ground from the pipe for each measurement line. For some measurement locations, the expected behavior was not seen and it was not possible to identify a clear resonance on the accelerance plot; for these locations, resonance data are not included (altogether, out of 126 measurement locations, the resonance was not identifiable in only seven instances).

For lines 1, 3, 5 and 6, the global minimum resonance frequency occurs directly above the pipe; for line 4, although the resonance frequency above the pipe is low, there are two other locations with similar values (at −0.2 m and +0.4 m); for line 2, the resonance frequency above the pipe is not amongst the lowest along the line.

It was thought that it might be possible to gain additional information by examining the magnitude of the accelerance at resonance. Magnitude data are shown in Fig. 10a–h (again the seven locations for which the resonance was not clear are not included).

Along two of the measurement lines (lines 1 and 3) the accelerance magnitude is a maximum directly above the pipe; on one line (line 5) the magnitude above the pipe is a minimum; for the remaining three lines (2, 4 and 6) no trends can be seen.

3.4. Discussion

From the discussion in Section 2.2.1, for the exciter used in these tests, one could expect to be able to detect objects buried at depths of the order of 10 cm. Whilst the results presented in
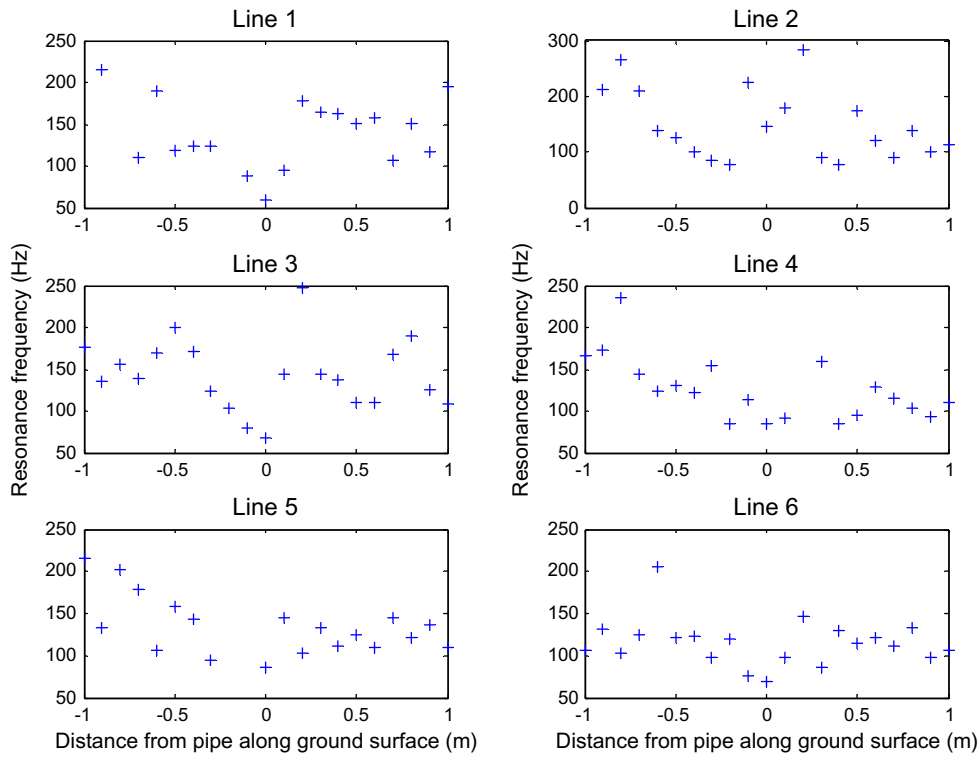
Fig. 9. Resonance frequencies along all six measurement lines (the line numbers correspond to those given in Fig. 6).
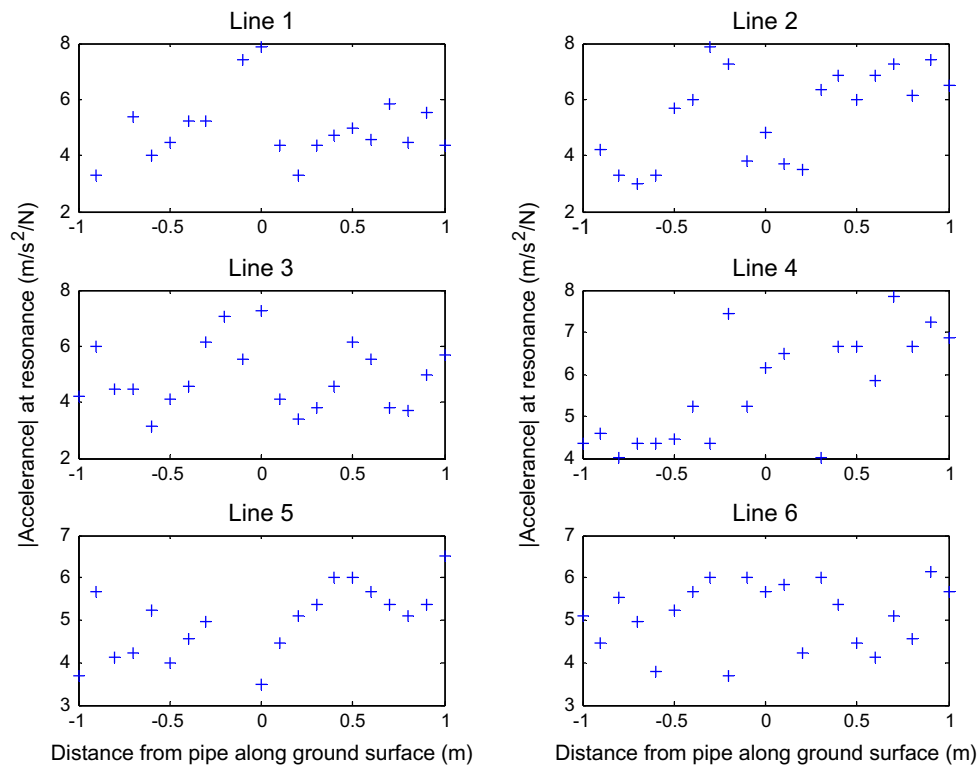

Fig. 10. Accelerance magnitude at resonance along all six measurement lines.

the previous section are not conclusive, that there is evidence that a pipe buried at ~30 cm can be detected is encouraging. The measurements indicate that, at least some of the time (>60% in this case), measuring the mass–spring resonance frequency, if not the peak magnitude, would serve as a useful indicator as to the location of a buried pipe.

4. Measurements on a live domestic waste

4.1. Description of experimental setup

Following on from the initial tests over the buried pipe rig, a further set of tests was carried out, this time in a rather different
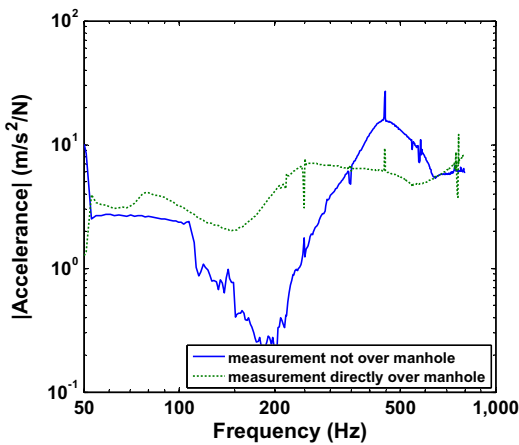
Fig. 11. Exposed drain cover.

Fig. 12. Two point accelerance measurements.

scenario. Measurements were made over a plastic manhole cover which gave access to a domestic wastepipe; directly beneath the manhole cover was an air-filled cavity extending down approxi-

mately 30 cm before reaching the waste pipe. The drain cover was not visible at the ground surface as it was covered with a layer of approximately 5 cm of gravel. Beneath the gravel around the manhole cover was a layer of stone paving; beneath that was the parent soil, similar to that in which the pipe rig was buried. Fig. 11 shows the drain cover with some of the gravel removed.

Clearly in this scenario, the ground does not resemble a homogeneous half-space as it did for the previous tests so, although the object to be detected (essentially an air cavity at a very shallow depth) ought to be easier to detect, the environment presents a greater challenge.

As for the previous tests the Wilcoxon electrodynamic shaker was used to excite the ground.

4.2. Point accelerance measurements

Point accelerance measurements were made along a 1.0 m long line traversing the manhole cover at its center. Measurements were made at approximately 10 cm intervals along the line, resulting in eleven measurement locations.

As before, a sweep input to the shaker was used, with a frequency range from 10 Hz to 800 Hz, and with a duration of approximately 30 s. A 2 kHz sampling rate was employed for the data acquisition, with a total acquisition time of 32.768 s.

For each measurement location, the point accelerance was again computed.

4.3. Results

Fig. 12 shows the point accelerance for one representative measurement location not directly above the manhole cover as well as one directly over it.

The mass–spring response can be clearly seen, with the resonance frequency at approximately 450 Hz, significantly higher than on the ground around the pipe. This is probably due to the high stiffness of the stone paving (and possibly gravel) compared with soil. Also shown in the figure is the point accelerance for the measurement point directly over the center of the manhole cover. Here it can be seen that the resonance frequency reduces
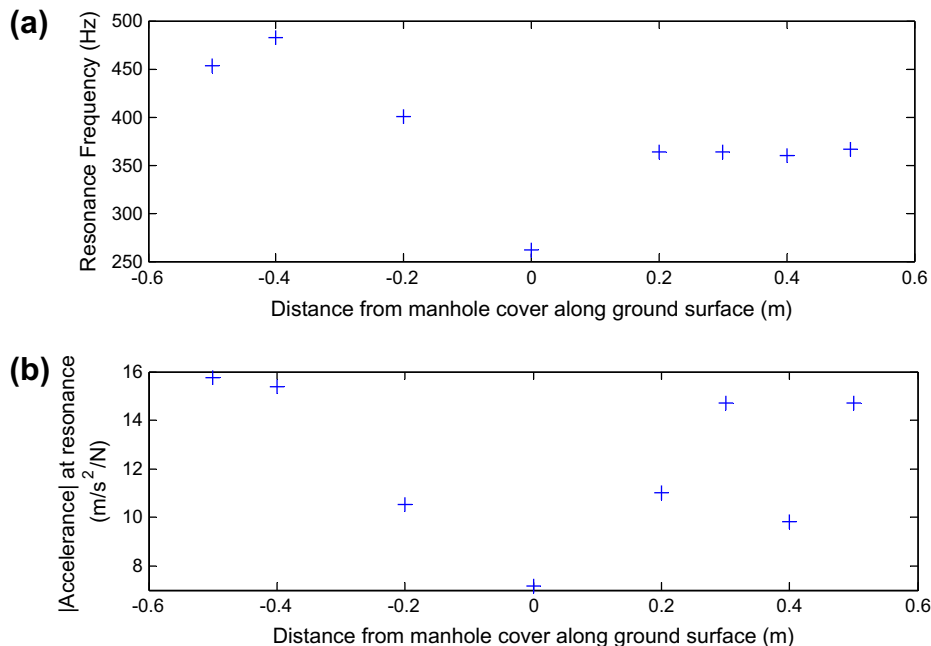

Fig. 13. (a) Resonance frequencies and (b) peak accelerance.

to around 250 Hz. The mass can be seen to change very slightly – close examination of the high-frequency, mass-controlled regions reveal a change from approximately 180–140 g – but again it is the stiffness which alters more. Here the mass seen over the manhole cover is the mass of the shaker piston alone, as expected (the mass of the manhole cover was only a few grammes); the additional 40 g seen in the other locations is slightly less than the expected radiation mass of around 80 g. The reduction in the peak height shows that over the manhole the damping increases. Fig. 13a and b shows the mass–spring resonance frequency plotted against distance along the ground from the manhole cover. As before, it was not possible to identify a clear resonance on all the accelerance plots, so for these locations, resonance data are not included (altogether, out of 11 measurement locations, the resonance was not identifiable in two instances).

Fig. 13a shows that above the manhole cover, the resonance frequency reduces significantly compared with adjacent locations. The diameter of the manhole cover was approximately 30 cm, so a lowered resonance frequency at the two locations either side of the center location would also be expected. This is indeed the case at 10 cm. Unfortunately at −10 cm no clear resonance could be observed.

From Fig. 13b, it can be seen that the magnitude of the accelerance at the resonance frequency decreases at the locations directly over the pipe.

4.4. Discussion

For these measurements the target object was at a depth (∼5 cm) well within the expected detection depth (∼10 cm). Furthermore, the target could be considered to be a straightforward one in that it was relatively large and the elastic properties of air differ significantly from those of the surrounding soil. However, the ground in the vicinity was definitely not homogeneous so it is encouraging that objects (albeit straightforward targets) can be located by making point measurements alone. Here both the resonance frequency and the peak magnitude were useful measures.

5. Conclusions

In this paper, the potential for making point accelerance measurements on the ground in order to detect shallow-buried objects, in particular pipes, has been explored. The theoretical background was discussed and it was shown that, at low frequencies, the ground behaves as a single-degree-of-freedom system with a well-defined resonance, the frequency of which will depend on the density and elastic properties of the soil locally. Expressions for the expected mass and stiffness components have been presented and how these might alter in the presence of a shallow-buried object discussed.

Preliminary measurements have been made on both a buried pipe rig and over a domestic waste pipe. For the buried pipe it was found that for four, possibly five, out of the six measurement lines crossing the pipe, the reduction in resonance frequency observed directly over the pipe would serve as a useful indicator as to the location of the pipe. The peak magnitude was found not to be a useful measure. For the measurements made over the manhole cover, both the resonance frequency and the peak magnitude revealed the location of the waste pipe.

The results presented here are preliminary and, whilst the findings are not conclusive, there is evidence to suggest that measuring point accelerance could serve as a useful adjunct to the more conventional methods of buried object detection, such as ground penetrating radar, for example. A particular advantage of the method is that the measurements are relatively quick to make and analyze; furthermore, they are straightforward to interpret. Importantly, modeling suggests that the detection depth depends on the excitation contact radius, so that greater detection depths could be achieved by using increased contact with the ground surface. Future work will examine this, along with the range of objects which can be detected with this technique.

References

Ashdown, C., 2000. Mains Location Equipment – A State of the Art Review and Future Research Needs. UKWIR Report (Reference Number 01/WM/06/1).

Gucunski, N., Krstic, V., Maher, A., 2000. Field implementation of the surface waves for obstacle detection (SWOD) method. In: Proc 15th World Conference on Nondestructive Testing, Roma, Italy.

Harding, J.W., Sneddon, N., 1945. The elastic stresses produced by the indentation of the plane surface of a semi-infinite elastic solid by a rigid punch. Proceedings of the Cambridge Philosophical Society 41 (1), 16–26.

Kinsler, L.E., Frey, A.R., Coppens, A.B., Sanders, J.V., 1982. Fundamentals of Acoustics, third ed. John Wiley & Sons, New York.

Mapping the Underworld, 2011. <http://www.mappingtheunderworld.ac.uk> (accessed July 2011).

McMahon, W., Burtwell, M.H., Evans, M., 2005. Minimising Street Works Disruption: The Real Costs of Street Works to the Utility Industry and Society. UK Water Industry Research, London, UK. UKWIR Report Number: 05/WM/12/8. ISBN:1-84057-408-9.

Miller, G.F., Pursey, H., 1954. The field and radiation impedance of mechanical radiators on the free surface of a semi-infinite isotropic solid. Proceedings of the Royal Society of London. Series A, Mathematical and Physical Sciences 223 (1155), 521–541.

Muggleton, J.M., Brennan, M.J., 2010. An assessment of laser vibrometry for the measurement of ground vibration. In: Proceedings of the 10th International Conference on Recent Advances in Structural Dynamics, 12–14 July 2010, Southampton, UK.

Pinnington, R.J., 1988. Approximate Mobilities of Built Up Structures. ISVR Technical Report 162, University of Southampton, UK.

Royal, A.C.D., Rogers C.D.F., Atkins P.R., Brennan, M.J., Chapman, D.N., Cohn, A.G., Curioni, G., Foo, K.Y., Goddard, K., Lewin, P.L., Metje, N., Muggleton, J.M., Naji, A., Pennock, S.R., Redfern, M.A., Saul, A.J., Swinger, S.G., Wang, P., 2010. Mapping the Underworld Phase II – Latest Developments International No-Dig 2010. In: 28th International Conference on the Trenchless Installation of Utilities, Singapore (8–10 November).

Royal, A.C.D., Atkins P.R., Brennan, M.J., Chapman, D.N., Chen, H., Cohn, A.G., Foo, K.Y., Goddard, K., Hayes, R., Hao, T., Lewin, P.L., Metje, N., Muggleton, J.M., Naji, A., Orlando, G., Pennock, S.R., Redfern, M.A., Saul, A.J., Swingler, S.G., Wang, P., Rogers C.D.F., 2011. Site assessment of multiple-sensor approaches for buried utility detection. Special issue on noninvasive sensing techniques and geophysical methods for cultural heritage and civil infrastructures monitoring. International Journal of Geophysics, Article ID 496123, 19pp. doi:10.1155/2011/496123.

Scott Jr., W.R., Schroder, C.T., Martin, J.S., Larson, G.D., 2001. Use of elastic waves for the detection of buried land mines. International Geoscience and Remote Sensing Symposium 3, 1116–1118.

Wilcoxon, 2011. Wilcoxon Shaker Specifications. <http://www.wilcoxon.com/vi_index.cfm?PD_ID=126> (accessed July 2011).

Xiang, N., Sabatier, J.M., 2002. Applications of acoustic-to-seismic coupling for landmine detection. In: Proc. International Symposium on Technology and the Mine Problem.

Xiang, N., Sabatier, J.M., 2003. An experimental study on antipersonnel landmine detection using acoustic to seismic coupling. Journal of the Acoustical Society of America 113 (3), 1333–1341.